ACS APPLIED MATERIALS & INTERFACES

Research Article

www.acsami.org

Growth and Properties of Hafnicone and HfO_2/Hafnicone Nanolaminate and Alloy Films Using Molecular Layer Deposition Techniques

Byoung H. Lee,[†] Virginia R. Anderson,[†] and Steven M. George*[,†,‡]

[†]Department of Chemistry and Biochemistry, [‡]Department of Mechanical Engineering, University of Colorado, Boulder, Colorado 80309-0215, United States

ABSTRACT: Molecular layer deposition (MLD) of the hafnium alkoxide polymer known as "hafnicone" was grown using sequential exposures of tetrakis(dimethylamido) hafnium (TDMAH) and ethylene glycol (EG) as the reactants. *In situ* quartz crystal microbalance (QCM) experiments demonstrated self-limiting reactions and linear growth versus the number of TDMAH/EG reaction cycles. *Ex situ* X-ray reflectivity (XRR) analysis confirmed linear growth and measured the density of the hafnicone films. The hafnicone growth rates were temperature-dependent and decreased from 1.2 Å per cycle at 105 °C to 0.4 Å per cycle at 205 °C. The measured density was ∼3.0 g/cm^3 for the hafnicone films at all temperatures. Transmission electron microscopy images revealed very uniform and conformal hafnicone films. The XRR studies also showed that the hafnicone films were very stable with time. Nanoindentation measurements determined that the elastic modulus and hardness of the hafnicone films were 47 ± 2 and 2.6 ± 0.2 GPa, respectively. HfO_2/hafnicone nanolaminate films also were fabricated using HfO_2 atomic layer deposition (ALD) and hafnicone MLD at 145 °C. The *in situ* QCM measurements revealed that HfO_2 ALD nucleation on the hafnicone MLD surface required at least 18 TDMAH/H_2O cycles. Hafnicone alloys were also fabricated by combining HfO_2 ALD and hafnicone MLD at 145 °C. The composition of the hafnicone alloy was varied by adjusting the relative number of TDMAH/H_2O ALD cycles and TDMAH/EG MLD cycles in the reaction sequence. The electron density changed continuously from 8.2×10^{23} e$^-$/cm^3 for pure hafnicone MLD films to 2.4×10^{24} e$^-$/cm^3 for pure HfO_2 ALD films. These hafnicone films and the HfO_2/hafnicone nanolaminates and alloys may be useful for flexible thin-film devices.

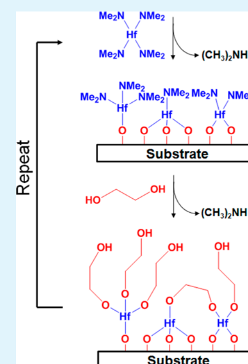

KEYWORDS: *molecular layer deposition, atomic layer deposition, hafnicone, HfO_2, nanolaminates, alloys*

I. INTRODUCTION

Molecular layer deposition (MLD) is a growth technique based on sequential and self-limiting surface reactions that deposits organic or hybrid organic−inorganic films.[1] MLD is very similar to atomic layer deposition (ALD), which has been developed for the deposition of many inorganic films.[2] These techniques allow the film thickness to be controlled at the atom or molecular fragment level. MLD techniques have been developed for depositing organic polymer films.[3−11] The organic precursors can also be combined with the inorganic ALD precursors to produce hybrid organic−inorganic materials.[1,12] One class of hybrid organic−inorganic MLD films that can be grown from metal precursors and various organic alcohols produces metal alkoxide polymer films known as the "metalcones."[12,13]

The first metalcone was the aluminum alkoxide polymer known as "alucone" that was grown using sequential exposures of trimethylaluminum (TMA) and ethylene glycol (EG) as the reactants.[14] Other alucone films have also been demonstrated using TMA, ethanolamine (EA), and maleic anhydride (MA) as the reactants to avoid the problem of double reactions that can inhibit film growth.[15] Zinc alkoxide polymers known as "zincones" were another type of metalcone grown using diethylzinc (DEZ) and EG as the reactants.[16,17] In addition, titanium alkoxide polymers known as "titanicones" can be grown using titanium tetrachloride and EG or glycerol as the reactants.[18] Zirconium alkoxide polymers known as "zircones" can also be grown using zirconium *tert*-butoxide and ethylene glycol as the reactants.[19] Other types of hybrid organic−inorganic MLD films can be also fabricated using various organometallic and organic precursors.[20−23]

Hybrid organic−inorganic films can also be deposited by combining ALD with MLD processes. The hybrid films can be grown by interspersing the ALD cycles and MLD cycles.[13] The composition of hybrid films can be tuned precisely by varying the relative number of ALD and MLD cycles. These hybrid films can be designated as "metalcone alloys." A representative metalcone alloy is an "alucone alloy" grown using Al_2O_3 ALD and alucone MLD.[24] The alucone alloy films display tunable density, refractive index, elastic modulus, and hardness as the alucone alloy is changed from the pure alucone MLD film to the pure Al_2O_3 ALD film.[24] Zircone alloy films also showed similar tunable properties by changing the ratio from pure zircone MLD film to pure ZrO_2 ALD film.[19] The ability to mix and match ALD and MLD methods offers a wide variety of

Received: July 5, 2014
Accepted: September 9, 2014
Published: September 9, 2014

ACS Publications © 2014 American Chemical Society

possibilities for tuning film composition, film structure, and film properties.

In this study, hafnicone film growth was investigated using tetrakis(dimethylamido) hafnium (TDMAH) and EG as the reactants.[13] Hafnicone films may be important as flexible thin films for dielectric and optical applications.[25] TDMAH is a very useful precursor having a high vapor pressure for HfO_2 ALD.[26] The sequential reactions of TDMAH and EG during MLD should form hafnium alkoxide polymeric films with a composition approximated by $(-Hf-O-R-O-)_n$, as shown in Figure 1.

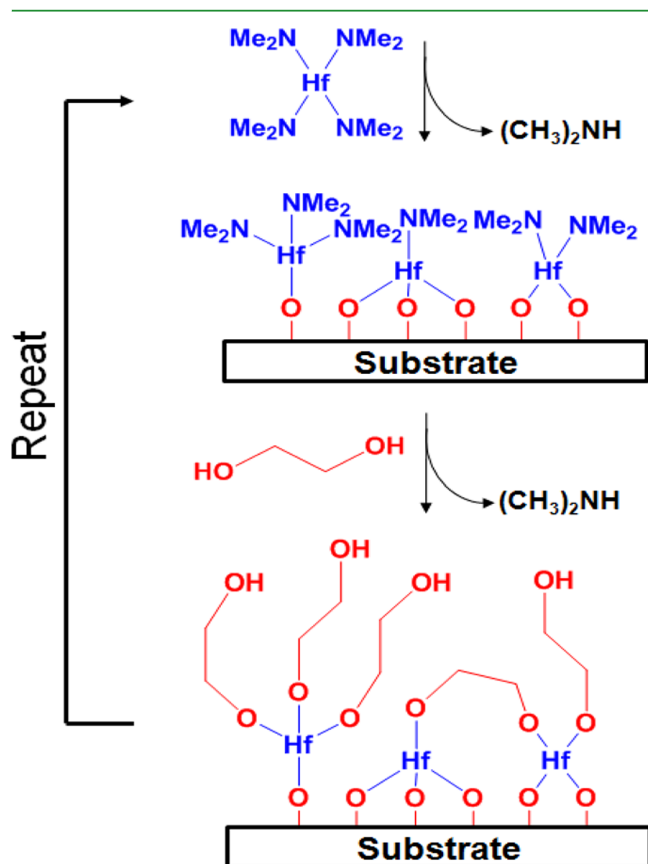

Figure 1. Schematic depicting the growth mechanism of hafnicone MLD film using TDMAH and EG.

In situ quartz crystal microbalance (QCM) measurements were used to monitor the self-limiting nature and growth mechanisms of the hafnicone film. X-ray reflectivity (XRR) was employed to determine the film thickness, density, and stability of the hafnicone films. Transmission electron microscopy (TEM) was also utilized to measure the structure and conformality of the hafnicone films. The properties of the hafnicone MLD film and HfO_2 ALD film were also compared using nanoindentation studies to measure the elastic modulus and hardness.

This study also explored the growth of HfO_2/hafnicone nanolaminates grown by combining HfO_2 ALD and hafnicone MLD processes at 145 °C. The HfO_2/hafnicone nanolaminates were investigated using *in situ* QCM analysis to examine the growth and nucleation during growth. TEM analysis was also employed to confirm the structure of the nanolaminates. Hafnicone alloys were also grown using HfO_2 ALD and hafnicone MLD at 145 °C. The composition of the hafnicone alloys was controlled by the relative ratio of the TDMAH/H_2O ALD cycles and TDMAH/EG MLD cycles. A wide range of electron densities were measured using XRR for hafnicone alloys with different compositions. These hafnicone alloys may also be tuned to control the refractive index, dielectric constant, elastic modulus, and hardness.

II. EXPERIMENTAL SECTION

The hafnicone and HfO_2/hafnicone nanolaminate and alloy films were fabricated using tetrakis(dimethylamido) hafnium ($Hf[N(CH_3)_2]_4$; 99.99%, Sigma-Aldrich) and ethylene glycol ($HO(CH_2)_2OH$; Reagent Plus >99%, Sigma-Aldrich) and water (H_2O, Fisher Scientific HPLC grade). Ultrahigh purity N_2 (Airgas) was used as the carrier gas in the viscous flow reactor and as the purge between reactant exposures. For *ex situ* analysis, the films were grown on boron doped p-type Si(100) substrates with a thin native oxide (Silicon Valley Microelectronics, Inc.). The sample substrates were cleaved from intact Si wafers into 1 in. × 1 in. squares. Degreasing was performed using a 15 min dip in Piranha solution (70% sulfuric acid and 30% hydrogen peroxide). The substrates were then rinsed with distilled H_2O and dried under N_2 gas.

The films were deposited in a viscous flow ALD reactor that has been described in detail elsewhere.[27] The hafnicone MLD films were deposited using a 0.2 s TDMAH dose, 60 s of purge, a 1 s EG dose, and 40 s of purge. The HfO_2 ALD films were deposited using a 0.2 s TDMAH dose, 60 s of purge, a 1 s H_2O dose, and 40 s of purge. The quartz crystal microbalance (QCM) measurements determined that these dose times were more than sufficient to saturate the surface reactions at all temperatures. The same deposition times were used at all temperatures for all experiments. The purge times were also long enough to ensure that no precursor was left in the reactor at the lower temperatures.

The HfO_2/hafnicone alloy films were deposited using alternating TDMAH (0.2 s)/H_2O (1 s) exposures for HfO_2 ALD and TDMAH (0.5 s)/EG (1 s) exposures for hafnicone MLD. The QCM measurements determined that these dose times were sufficient to saturate the surface at the growth temperature of 145 °C. The hafnicone alloys were defined by the ratio of ALD/MLD cycles. For example, the 1:1 hafnicone alloy was grown using an alternation of one cycle of HfO_2 ALD and one cycle of hafnicone MLD. In comparison, the 2:1 hafnicone alloy was grown using an alternation of two cycles of HfO_2 ALD and one cycle of hafnicone MLD. The reactant sequence for the formation of the 2:1 hafnicone alloy is TDMAH/H_2O/TDMAH/H_2O/TDMAH/EG.

The *in situ* QCM measurements were performed in the viscous flow reactor using a Maxtek TM400 thin film deposition monitor.[27] The QCM sensors were quartz crystals with a polished Au face and a 6 MHz oscillation frequency (Colorado Crystal Corp.). The crystals were sealed into a Maxtek BSH-150 bakeable crystal housing and purged during deposition to avoid growth on the back side. During growth, the QCM was positioned horizontally and facing downward in the middle of the reactor.

The thicknesses and densities of the hafnicone and hafnicone alloy films were determined by X-ray reflectivity (XRR) analysis. These films were deposited on boron-doped p-type Si(100) substrates. The XRR analysis was performed using a Bede D1 high-resolution X-ray diffractometer from Bede Scientific, Inc. The diffractometer was equipped with a Cu Kα X-ray tube with a wavelength of 1.54 Å. A filament current of 35 mA and a voltage of 40 kV were used for the measurements. For each sample, an ω-2θ scan was performed using a 10 arcsec step size from 300 to 6000 arcsec. The XRR data was fit using the REFS fitting software from Bede Scientific, Inc., to extract the thickness, density, and roughness of the hafnicone and hafnicone alloy samples.

Transmission electron microscope (TEM) images were obtained by Prof. M. M. Sung's laboratory at Hanyang University. The specimen for cross-sectional TEM studies was prepared by mechanical grinding and polishing to obtain a sample thickness of ~10 μm. This treatment was followed by argon ion milling using a Gatan precision ion

polishing system (PIPSTM, Model 691). The TEM image was acquired with a JEOL-2100F transmission electron microscope.

The refractive index n of hafnicone film was obtained from *ex situ* reflective spectroscopic ellipsometry investigations. These measurements were performed using a J. A. Woollam M-2000 spectroscopic ellipsometer employing a spectral range from 240 to 1700 nm with an incidence angle of 75°. The refractive index values were derived from ellipsometric parameters for hafnicone films deposited on silicon substrates using a Cauchy model.

Indentation of the hafnicone films was performed at room temperature using a nanoindenter (Nano Dynamic Contact Module (DCM), Agilent Technologies, Inc.) equipped with a diamond Berkovich tip.[28] These indentation measurements characterized the elastic modulus and the hardness of MLD films. Material properties were evaluated according to the Oliver−Pharr method. The Oliver−Pharr method used in conjunction with the continuous stiffness method (CSM) can characterize specimens over a range of thicknesses.[29,30] The nanoindentation technique is accurate to within about 5−10% of the actual values. Accuracy improves with the averaging of multiple indentations.

Hafnicone films with thicknesses of ∼100 nm were deposited onto the Si(100) wafers at 145 °C. Immediately prior to indentation, the nanoindenter was calibrated using fused silica to determine the area coefficients for the tip. Indents were performed up to a depth of 50 nm at a constant loading rate of 0.05 s^{-1}. The maximum load was held for 10 s for stabilization and then rapidly unloaded at a rate of 250 $\mu N\ s^{-1}$. The load was also held at 1% of the maximum load for 30 s to obtain a thermal drift correction. For all indentation experiments, test locations were separated by 100 μm to ensure isolation between the 10 test sites.

Because of surface roughness effects[31] and difficulties calibrating the tip area function,[32] artifacts are often observed in nanoindentation measurements of the hardness and elastic modulus for small indentation depths of <10−15 nm.[33] To avoid these artifacts, the property values were averaged at depths between 25 and 35 nm into the film. The property values were constant at penetration depths >15 nm into the film. This constancy argues that substrate effects are minimal.[34]

III. RESULTS AND DISCUSSION

1. Growth of Hafnicone MLD Film. *In situ* QCM measurements were used to confirm the self-limiting behavior of both the TDMAH and EG reactions during hafnicone MLD. Figure 2a shows the mass gain versus the TDMAH exposure time at 145 °C. For these experiments, the EG exposure time was maintained at 1 s. The timing sequence during the hafnicone MLD was x-60−1−40, where x was the TDMAH exposure time. The maximum mass gain of 17 ng/cm^2 was observed for TDMAH exposure times >0.1 s. This behavior shows that the TDMAH reaction is self-limiting and no further reaction occurs with larger TDMAH exposures. A TDMAH exposure time of 0.2 s was used for all additional experiments to ensure the TDMAH reaction reached completion.

Figure 2b displays the mass gain versus the EG exposure at 145 °C. The timing sequence during the hafnicone MLD was 0.2−60-y-40, where y was the EG exposure time. Figure 2b indicates that the mass gain reaches completion for EG exposure times >1 s. This behavior shows that the EG reaction is self-limiting and no further reaction occurs with larger EG exposures. An EG exposure time of 1 s was used for all additional experiments to ensure the EG reaction reached completion.

Figure 3a shows the linear mass gain monitored by the QCM during 100 cycles of hafnicone MLD with alternating exposures of TDMAH and EG at 145 °C. The timing sequence during one MLD cycle was 0.2−60−1−40. The initial HfO_2 surface was grown using 100 cycles of HfO_2 ALD using TDMAH and

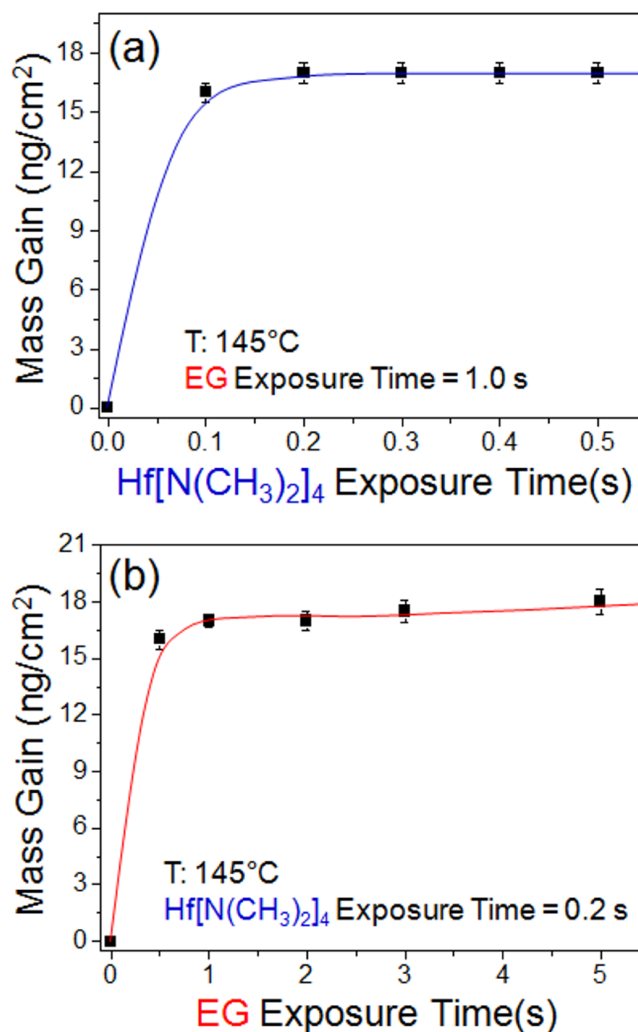

Figure 2. Mass gains per cycle during hafnicone MLD at 145 °C versus (a) TDMAH exposure time with reactant timing sequence of x-60−1−40 and (b) EG exposure time with a reactant timing sequence of 0.2−60-y-60.

H_2O at 145 °C. In the first two MLD cycles on the HfO_2 ALD surface, large positive mass gains were obtained for both TDMAH and EG exposures. These large mass gains result from the large number of reactive sites on the metal oxide surface. After the initial nucleation regime, the mass gain per cycle was ∼17 ng/cm^2/cycle and was very reproducible.

The details of the QCM mass gains during the individual TDMAH and EG exposures during hafnicone MLD at 145 °C are displayed in Figure 3b. The TDMAH exposure results in a mass gain of ∼17 ng/cm^2, and the mass gain after the EG exposure was negligible. The mass gains were consistent from cycle to cycle for both TDMAH and EG exposures at all temperatures.

Hafnicone films were grown on silicon wafers that had a native SiO_2 oxide. XRR data was recorded for various numbers of AB cycles ranging from 100 to 500 cycles at 145 °C. The reaction timing sequence was 0.2−60−1−40. The XRR scans displayed an oscillatory intensity as a function of the angle that was consistent with very smooth and high quality hafnicone films. Figure 4 shows the film thickness versus number of AB cycles for hafnicone film growth obtained from the XRR scans. The XRR scans were fit to account for the hafnicone film and

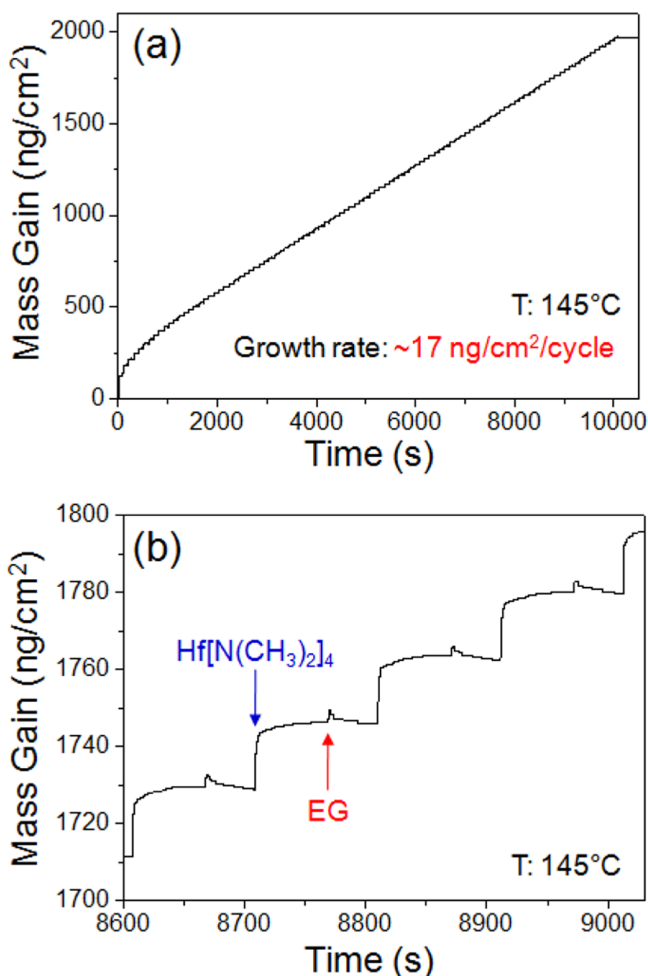

Figure 3. (a) Mass gain versus time during 100 cycles of hafnicone MLD on HfO_2 at 145 °C. The linear growth rate is ~17 ng/(cm^2 cycle). (b) Four reaction cycles during hafnicone MLD in the steady state growth regime of Figure 3a.

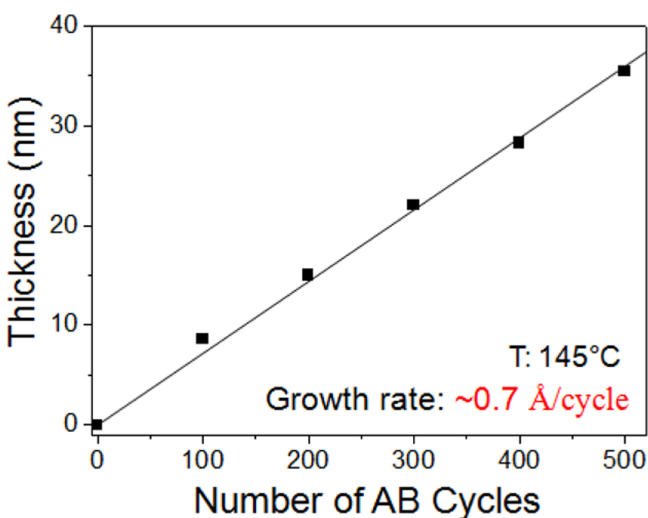

Figure 4. Film thickness versus number of AB cycles for hafnicone MLD at 145 °C obtained from XRR data.

the native SiO_2 film on the Si wafer. The film thickness versus number of MLD cycles is extremely linear and consistent with a growth rate of ~0.7 Å per MLD cycle at 145 °C.

To investigate the stability of the hafnicone film in air, a hafnicone film grown using 500 cycles was deposited on a silicon substrate using alternating TDMAH and EG exposures at 145 °C. XRR scans were then recorded after deposition and after a time delay of 5 days following deposition. The XRR scans were equivalent. This constancy argues that the hafnicone films are very stable in air.

The temperature dependence of the hafnicone growth rate per cycle was explored by depositing 500 AB cycles with a timing sequence of 0.2−60−1−40. Figure 5 shows the growth rate and the film density at deposition temperatures from 105 to 205 °C. There is not a temperature range over which the growth rate is constant. The growth rate gradually decreases from 1.2 Å/cycle at 105 °C to 0.4 Å/cycle at 205 °C. The decrease in the hafnicone MLD growth rate versus deposition temperature can be partly attributed to the greater number of double reactions for EG at higher temperatures.[16] Similar temperature dependences have been observed previously for alucone and zincone MLD.[14,16] The measured film densities were independent of the deposition temperature and were constant at ~3.0 g/cm^3. These measured densities of the hafnicone films are much less than the density of ~9.4 g/cm^3 for pure HfO_2 ALD films.

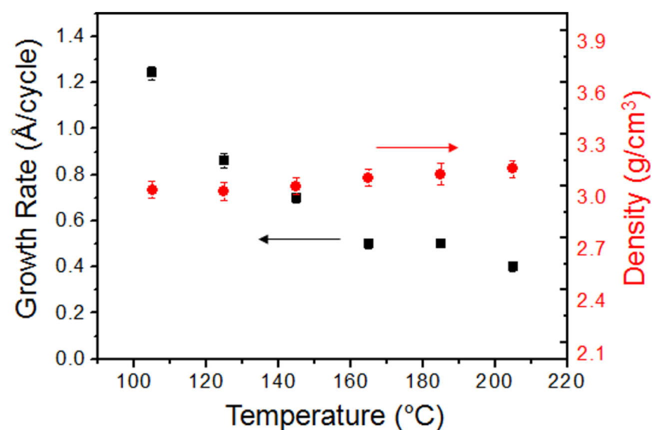

Figure 5. Growth per cycle and density for hafnicone MLD films versus deposition temperature.

Figure 6 displays a cross-sectional transmission electron microscopy (TEM) image of a HfO_2/hafnicone/HfO_2 trilayer that was deposited on a Si(100) substrate at 145 °C. The hafnicone film was sandwiched between two HfO_2 ALD layers for image contrast. The TEM image clearly shows a lighter hafnicone film with smooth interfaces. The hafnicone film is conformal on the HfO_2 ALD layer on the Si substrate. The measured film thickness of the hafnicone film was ~10 nm. This thickness is in approximate agreement with the growth rate measured by XRR in Figure 4.

Figure 7 displays the refractive indices for the HfO_2 ALD and hafnicone MLD films grown at 145 °C obtained from the spectroscopic ellipsometry measurements. The higher density for the HfO_2 ALD films leads to a much higher refractive index for the HfO_2 ALD film compared with the hafnicone MLD films. The refractive indices for HfO_2 ALD and hafnicone MLD films at λ = 589 nm (Na D-line) are n = 2.05 and n = 1.62, respectively. The refractive index of n = 2.05 for the HfO_2 ALD films is in good agreement with previous measurements. A refractive index of n = 2.07−2.08 at 540 nm was obtained for HfO_2 ALD films grown at 275 °C using TDMAH and H_2O.[26]

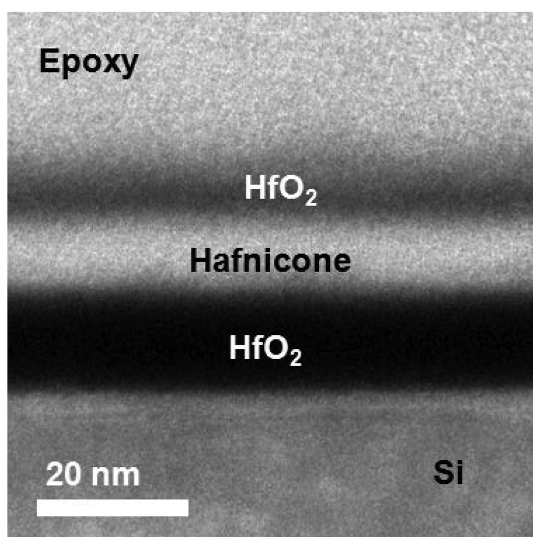

Figure 6. TEM image of hafnicone MLD film sandwiched between two HfO_2 ALD films.

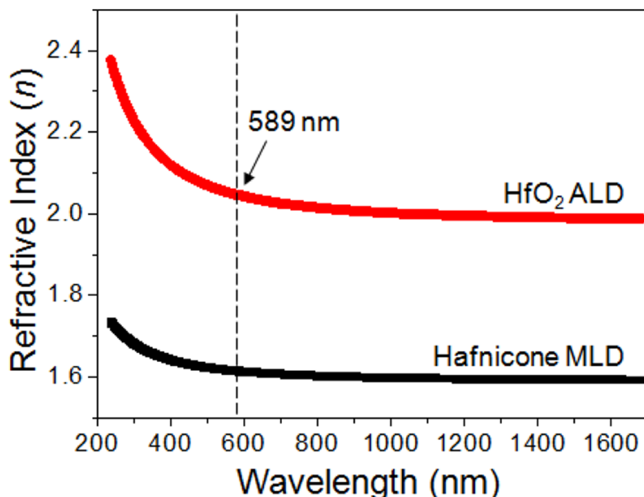

Figure 7. Refractive index for HfO_2 ALD and hafnicone MLD versus wavelength. HfO_2 ALD and hafnicone MLD films were grown at 145 °C.

A refractive index of n = 2.08 at 580 nm was measured for HfO_2 ALD films grown at 150 °C using tetrakis(ethylmethylamido) hafnium and H_2O.[35]

The refractive index of n = 1.62 for hafnicone MLD films at λ = 589 nm can be compared with the refractive indices of other metalcone films. Alucone MLD films have a smaller refractive index of n = 1.50.[14] Zircone MLD films have a similar refractive index of 1.63.[19] Titanicone MLD films have larger refractive indices of n = 1.7 or n = 1.8 using ethylene glycol or glycerol, respectively, as the organic reactant.[18] The refractive indices of the various metalcone films scale approximately with the refractive indices of their parent metal oxide.

Elastic modulus and hardness of hafnicone films were determined using nanoindentation techniques. Figure 8 shows nanoindentation results for hafnicone films with a thickness of ∼100 nm grown using TDMAH and EG at 145 °C. For comparison, HfO_2 ALD film with the same thickness of ∼100 nm were also grown using TDMAH and H_2O at 145 °C. Analysis of the data demonstrates that the hafnicone films have

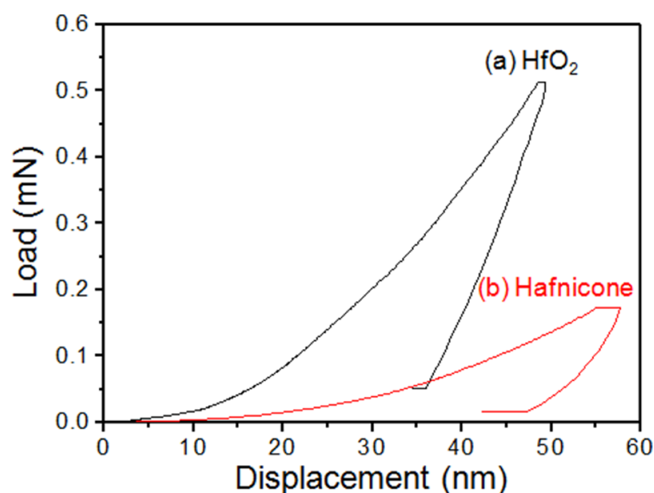

Figure 8. Load vs displacement curves from nanoindentation measurements for (a) pure HfO_2 ALD and (b) hafnicone MLD films grown at 145 °C.

an elastic modulus of 47 ± 2 GPa and a hardness of 2.6 ± 0.2 GPa. In comparison, the HfO_2 ALD films have an elastic modulus of 220 ± 20 GPa and a hardness of 13 ± 2.5 GPa.

The mechanical parameters for the HfO_2 ALD films are in good agreement with previous measurements for HfO_2 ALD films grown using tetrakis(ethylmethylamido) hafnium and H_2O at 250 °C. These earlier measurements determined an elastic modulus of 220 ± 40 GPa and a hardness of 9.5 ± 2 GPa.[36] The elastic modulus of 47 ± 2 GPa for the hafnicone film can be compared with the elastic moduli of other metalcone films. Alucone films have a smaller elastic modulus of 21 ± 8 GPa.[24] Zircone films also have a smaller elastic modulus of 27 ± 0.6 GPa.[19] Titanicone films have an elastic modulus that is very different and dependent on the organic reactant. An elastic modulus of 30.6 ± 0.1 GPa was obtained using glycerol as the organic reactant.[18] A much smaller elastic modulus of 8.0 ± 0.4 GPa was measured using ethylene glycol as the organic reactant.[18] The size of these elastic moduli may be dependent on the bonding and cross-linking in the metalcone.

2. Growth of HfO_2/Hafnicone Nanolaminates and Alloys. Hafnicone MLD can be combined with HfO_2 ALD to obtain nanolaminates or alloys. The HfO_2/hafnicone nanolaminates and hafnicone alloys can be deposited using alternating TDMAH (0.2 s)/H_2O (1 s) exposures for HfO_2 ALD and TDMAH (0.5 s)/EG (1 s) exposures for hafnicone MLD at 145 °C. Figure 9a displays the growth of HfO_2/hafnicone nanolaminates grown using the repetition of 40 cycles of HfO_2 ALD and 40 cycles of hafnicone MLD at 145 °C. Zones I and II show HfO_2 ALD and hafnicone MLD mass gains, respectively, versus time. These QCM measurements demonstrate that HfO_2/hafnicone nanolaminates can be grown progressively by sequential ALD and MLD processes. In addition, the growth is repeatable for each HfO_2/hafnicone bilayer in the HfO_2/hafnicone nanolaminate.

Figure 9b shows the mass gain during 40 cycles of HfO_2 ALD on HfO_2 ALD and hafnicone MLD surfaces. HfO_2 ALD on the HfO_2 ALD surface proceeds linearly from the start of the 40 cycles. In contrast, there are nucleation delays for HfO_2 ALD on the hafnicone MLD surface. During the first 18 TDMAH/H_2O cycles, the mass gain for HfO_2 ALD gradually increases with increasing number of TDMAH/H_2O cycles. Subsequently,

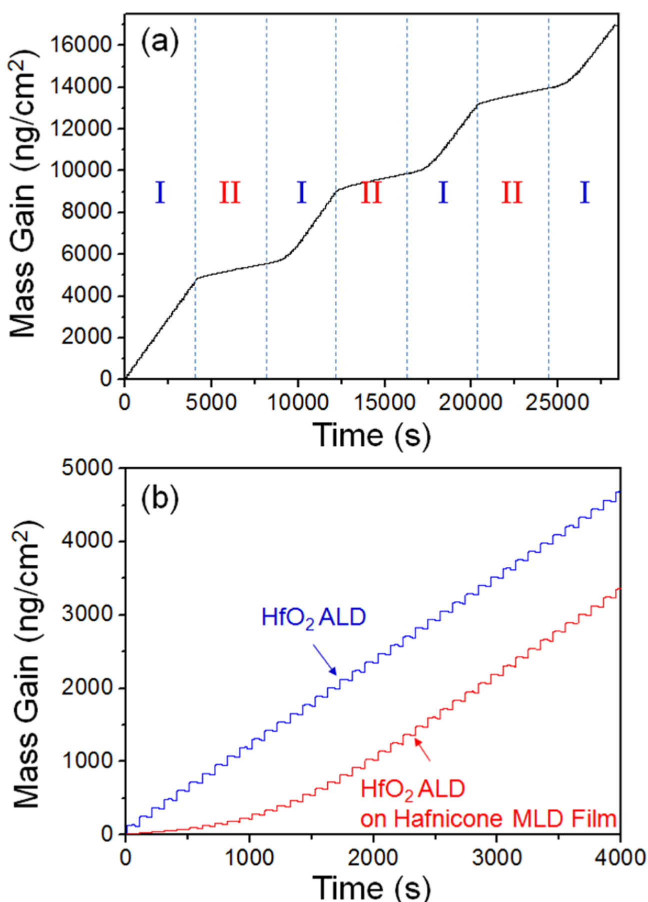

Figure 9. (a) Mass gain versus time during growth at 145 °C of HfO_2 (I)/hafnicone MLD (II) nanolaminate on HfO_2 ALD film. (b) Mass gain versus time for 40 cycles of HfO_2 ALD on HfO_2 ALD film and 40 cycles of HfO_2 ALD on hafnicone MLD film.

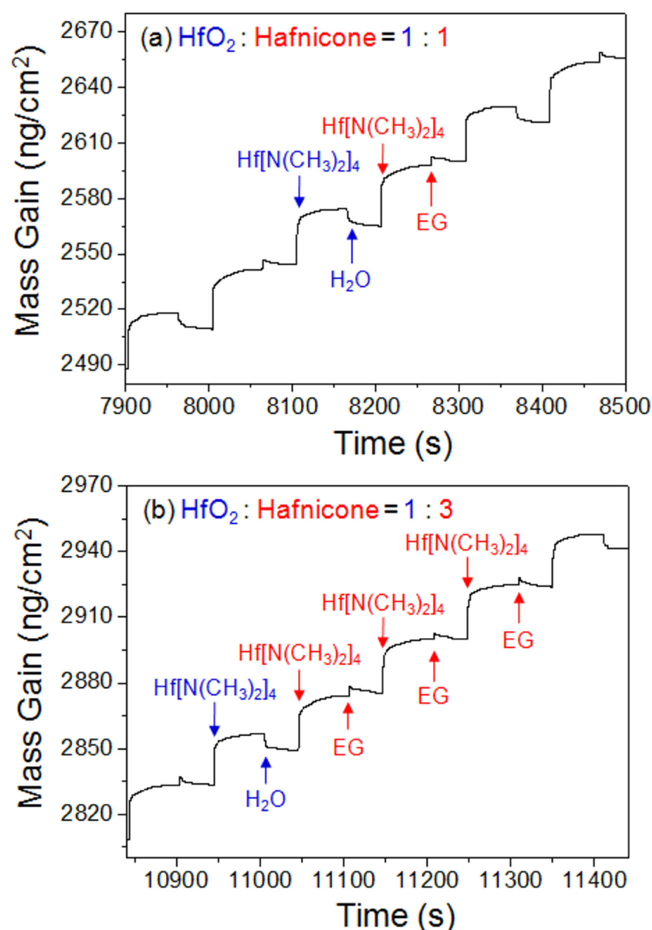

Figure 10. (a) Mass gain versus number of sequences at 145 °C for the growth of the 1:1 hafnicone alloy film in the steady state regime. (b) Mass gain versus number of sequences at 145 °C for the growth of the 1:3 hafnicone alloy film in the steady state regime.

a linear HfO_2 ALD growth rate is reached with an average growth rate of 111 ng/cm^2 per TDMAH/H_2O cycle. This increasing HfO_2 ALD growth rate with number of HfO_2 ALD cycles is attributed to a progressive increase in surface sites as the HfO_2 ALD process establishes itself on the hafnicone MLD surface.

Hafnicone alloy growth using HfO_2 ALD and hafnicone MLD was also studied using *in situ* QCM investigations at 145 °C. Figure 10 displays QCM results for the growth of the 1:1 and 1:3 hafnicone alloys at 145 °C. All timing sequences for the ALD and MLD reactions were (0.2, 60, 1, 40). Figure 10a shows the mass gain versus time in the linear steady-state growth regime for the 1:1 hafnicone alloy. The 1:1 hafnicone alloy film growth is characterized by consistent mass gains after the TDMAH, H_2O, TDMAH, and EG exposures. For the growth of the 1:1 hafnicone alloy, mass gains of +29, −8, +32, and +3 ng/cm^2 are observed during the TDMAH, H_2O, TDMAH, and EG exposures, respectively. The 1:1 hafnicone alloy had a growth rate of ∼56 ng/(cm^2 sequence).

Figure 10b also shows the mass gain versus time in the linear steady-state growth regime for the 1:3 hafnicone alloy growth at 145 °C. The growth of the 1:3 hafnicone alloy film displays consistent mass gains after the TDMAH, H_2O, and EG exposures. The 1:3 hafnicone alloy had a growth rate of ∼90 ng/(cm^2 sequence).

The fraction of organic and inorganic constituents in the hafnicone alloy film can be controlled by varying the number of HfO_2 ALD and hafnicone MLD cycles used to grow the hafnicone alloy film. As the fraction of inorganic constituent increases, the density, refractive index, elastic modulus, and hardness are all expected to increase.[24] Consistent with these expectations, the density of hafnicone alloy films increases with the fraction of HfO_2 ALD cycles in the exposure sequence measured by (ALD cycles)/(ALD + MLD cycles). Figure 11 presents the electron density values derived from the XRR scans for hafnicone alloys grown at 145 °C with different ALD/MLD ratios.

The electron densities in Figure 11 vary from 8.2×10^{23} e^-/cm^3 for pure hafnicone MLD films to 2.4×10^{24} e^-/cm^3 for pure HfO_2 ALD films. Assuming compositions of −HfO-$(CH_2)_2$O− for hafnicone and HfO_2 for HfO_2, the mass densities of the pure hafnicone film and HfO_2 film are ∼3.0 and ∼9.4 g/cm^3, respectively. For the hafnicone alloys, the density increases gradually and relatively smoothly with increasing percentage of ALD cycles/[ALD+MLD cycles]. This result indicates that the density of the hafnicone alloy films can be precisely tuned by varying the relative number of TDMAH/H_2O and TDMAH/EG cycles during the hafnicone alloy film growth. Similar tuning could be expected for the refractive index, dielectric constant, elastic modulus, and hardness.

dx.doi.org/10.1021/am504341r | ACS Appl. Mater. Interfaces 2014, 6, 16880−16887

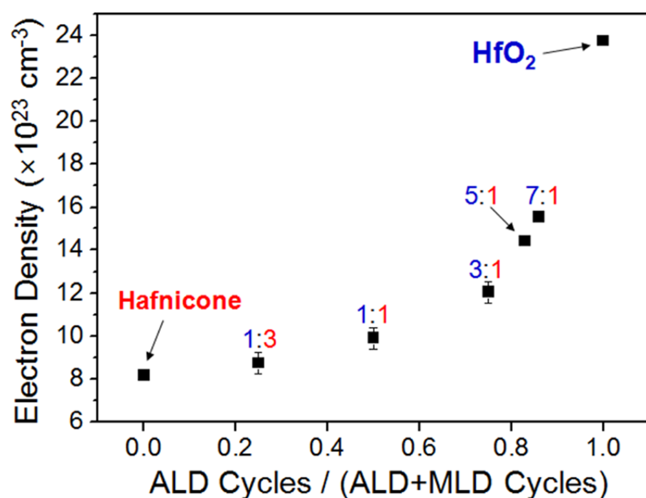

Figure 11. Electron density versus ALD cycles/[ALD+MLD cycles] for the hafnicone alloy films grown at 145 °C.

IV. CONCLUSIONS

Hafnicone films were fabricated using molecular layer deposition (MLD) techniques with tetrakis(dimethylamido) hafnium (TDMAH) and ethylene glycol (EG) as the reactants. The hafnicone films grew linearly with number of reaction cycles and displayed self-limiting growth versus the TDMAH and EG reaction exposures. The hafnicone growth rates decreased versus growth temperature from 1.2 Å per cycle at 105 °C to 0.4 Å per cycle at 205 °C. The density of the hafnicone films was ~3.0 g/cm^3 for all growth temperatures. Uniform and conformal hafnicone films were observed by TEM images.

HfO_2 atomic layer deposition (ALD) and hafnicone MLD were combined to fabricate HfO_2/hafnicone nanolaminates and alloys at 145 °C. The QCM measurements showed that HfO_2 ALD nucleation on hafnicone MLD films required at least 18 TDMAH/H_2O cycles. In comparison, hafnicone MLD proceeded rapidly on HfO_2 ALD films with no nucleation delay. The TEM images showed very well-defined HfO_2/hafnicone nanolaminated films.

Hafnicone alloy films were also fabricated by combining HfO_2 ALD and hafnicone MLD. Hafnicone alloys were grown using relative numbers of HfO_2 ALD and hafnicone MLD cycles varying from 1:3 to 7:1 ((TDMAH/H_2O)/(TDMAH/EG)). The electron density varied from 8.2×10^{23} e$^-$/cm^3 for pure hafnicone MLD films to 2.4×10^{24} e$^-$/cm^3 for pure HfO_2 ALD films. These results indicate that hafnicone alloy films could be employed to provide tunable refractive index, dielectric constant, elastic modulus, and hardness. The hafnicone and HfO_2/hafnicone nanolaminate and alloy films should be useful for many functional flexible film applications.

AUTHOR INFORMATION

Corresponding Author

*E-mail: Steven.George@colorado.edu.

Notes

The authors declare no competing financial interest.

ACKNOWLEDGMENTS

This research was funded by the National Science Foundation (CHE-1306131). We thank Prof. M. M. Sung and his laboratory at Hanyang University for obtaining the TEM images.

REFERENCES

(1) George, S. M.; Yoon, B.; Dameron, A. A. Surface Chemistry for Molecular Layer Deposition of Organic and Hybrid Organic-Inorganic Polymers. *Acc. Chem. Res.* **2009**, *42*, 498−508.
(2) George, S. M. Atomic Layer Deposition: An Overview. *Chem. Rev.* **2010**, *110*, 111−131.
(3) Adamczyk, N. M.; Dameron, A. A.; George, S. M. Molecular Layer Deposition of Poly(p-phenylene terephthalamide) Films Using Terephthaloyl Chloride and p-Phenylenediamine. *Langmuir* **2008**, *24*, 2081−2089.
(4) Du, Y.; George, S. M. Molecular Layer Deposition of Nylon 66 Films Examined Using in situ FTIR Spectroscopy. *J. Phys. Chem. C* **2007**, *111*, 8509−8617.
(5) Kim, A.; Filler, M. A.; Kim, S.; Bent, S. F. Layer-by-Layer Growth on Ge(100) via Spontaneous Urea Coupling Reactions. *J. Am. Chem. Soc.* **2005**, *127*, 6123−6132.
(6) Lee, J. S.; Lee, Y. J.; Tae, E. L.; Park, Y. S.; Yoon, K. B. Synthesis of Zeolite as Ordered Multicrystal Arrays. *Science* **2003**, *127*, 818−821.
(7) Li, Y. H.; Wang, D.; Buriak, J. M. Molecular Layer Deposition of Thiol-Ene Multilayers on Semiconductor Surfaces. *Langmuir* **2010**, *26*, 1232−1238.
(8) Loscutoff, P. W.; Lee, H. B. R.; Bent, S. F. Deposition of Ultrathin Polythiourea Films by Molecular Layer Deposition. *Chem. Mater.* **2010**, *22*, 5563−5569.
(9) Putkonen, M.; Harjuoja, J.; Sajavaara, T.; Niinisto, L. Atomic Layer Deposition of Polyimide Thin Films. *J. Mater. Chem.* **2007**, *17*, 664−669.
(10) Shao, H. L.; Umemoto, S.; Kikutani, T.; Okui, N. Layer-by-Layer Polycondensation of Nylon 66 by Alternating Vapour Deposition Polymerization. *Polymer* **1997**, *38*, 459−462.
(11) Yoshimura, T.; Tatsuura, S.; Sotoyama, W.; Matsuura, A.; Hayano, T. Quantum Wire and Dot Formation by Chemical Vapor Deposition and Molecular Layer Deposition of One-Dimensional Conjugated Polymer. *Appl. Phys. Lett.* **1992**, *60*, 268−270.
(12) George, S. M.; Lee, B. H.; Yoon, B.; Abdulagatov, A. I.; Hall, R. A. Metalcones: Hybrid Organic-Inorganic Films Fabricated Using Atomic & Molecular Layer Deposition Techniques. *J. Nanosci. Nanotechnol.* **2011**, *11*, 7956−7961.
(13) Lee, B. H.; Yoon, B.; Abdulagatov, A. I.; Hall, R. A.; George, S. M. Growth and Properties of Hybrid Organic-Inorganic Metalcone Films Using Molecular Layer Deposition Techniques. *Adv. Funct. Mater.* **2013**, *23*, 532−546.
(14) Dameron, A. A.; Seghete, D.; Burton, B. B.; Davidson, S. D.; Cavanagh, A. S.; Bertrand, J. A.; George, S. M. Molecular Layer Deposition of Alucone Polymer Films Using Trimethylaluminum and Ethylene Glycol. *Chem. Mater.* **2008**, *20*, 3315−3326.
(15) Yoon, B.; Seghete, D.; Cavanagh, A. S.; George, S. M. Molecular Layer Deposition of Hybrid Organic-Inorganic Alucone Polymer Films Using a Three-Step ABC Reaction Sequence. *Chem. Mater.* **2009**, *21*, 5365−5374.
(16) Yoon, B.; O'Patchen, J. L.; Seghete, D.; Cavanagh, A. S.; George, S. M. Molecular Layer Deposition of Hybrid Organic-Inorganic Polymer Films using Diethylzinc and Ethylene Glycol. *Chem. Vap. Deposition* **2009**, *15*, 112−121.
(17) Peng, Q.; Gong, B.; VanGundy, R. M.; Parsons, G. N. "Zincone" Zinc Oxide-Organic Hybrid Polymer Thin Films Formed by Molecular Layer Deposition. *Chem. Mater.* **2009**, *21*, 820−830.
(18) Abdulagatov, A. I.; Hall, R. A.; Sutherland, J. L.; Lee, B. H.; Cavanagh, A. S.; George, S. M. Molecular Layer Deposition of Titanicone Films using $TiCl_4$ and Ethylene Glycol or Glycerol: Growth and Properties. *Chem. Mater.* **2012**, *24*, 2854−2863.
(19) Lee, B. H.; Anderson, V. R.; George, S. M. Molecular Layer Deposition of Zircone and ZrO_2/Zircone Alloy Films: Growth and Properties. *Chem. Vap. Deposition* **2013**, *19*, 204−212.
(20) Lee, B. H.; Ryu, M. K.; Choi, S.; Lee, K. H.; Im, S.; Sung, M. M. Rapid Vapor-Phase Fabrication of Organic-Inorganic Hybrid Super-

lattices with Monolayer Precision. *J. Am. Chem. Soc.* **2007**, *129*, 16034−16041.
(21) Lee, B. H.; Im, K. K.; Lee, K. H.; Im, S.; Sung, M. M. Molecular Layer Deposition of ZrO_2-based Organic-Inorganic Nanohybrid Thin Films for Organic Thin Film Transistors. *Thin Solid Films* **2009**, *517*, 4056−4060.
(22) Cho, S.; Han, G.; Kim, K.; Sung, M. M. High-Performance Two-Dimensional Polydiacetylene with a Hybrid Inorganic-Organic Structure. *Angew. Chem., Int. Ed.* **2011**, *50*, 2742−2746.
(23) Sundberg, P.; Sood, A.; Liu, X. W.; Johansson, L. S.; Karppinen, M. Atomic/Molecular Layer Deposited Thin-Film Alloys of Ti-4,4′-Oxydianiline Hybrid-TiO_2 with Tunable Properties. *Dalton Trans.* **2012**, *41*, 10731−10739.
(24) Lee, B. H.; Yoon, B.; Anderson, V. R.; George, S. M. Alucone Alloys with Tunable Properties Using Alucone Molecular Layer Deposition and Al_2O_3 Atomic Layer Deposition. *J. Phys. Chem. C* **2012**, *116*, 3250−3257.
(25) Robertson, J. High Dielectric Constant Gate Oxides for Metal Oxide Si Transistors. *Rep. Prog. Phys.* **2006**, *69*, 327−396.
(26) Hackley, J. C.; Gougousi, T. Properties of Atomic Layer Deposited HfO_2 Thin Films. *Thin Solid Films* **2009**, *517*, 6576−6583.
(27) Elam, J. W.; Groner, M. D.; George, S. M. Viscous Flow Reactor with Quartz Crystal Microbalance for Thin Film Growth by Atomic Layer Deposition. *Rev. Sci. Instrum.* **2002**, *73*, 2981−2987.
(28) Miller, D. C.; Foster, R. R.; Jen, S.; Bertrand, J. A.; Seghete, D.; Yoon, B.; Lee, Y.; George, S. M.; Dunn, M. L. Thermomechanical Properties of Aluminum Alkoxide (Alucone) Films Created Using Molecular Layer Deposition. *Acta Mater.* **2009**, *57*, 5083−5092.
(29) Oliver, W. C.; Pharr, G. M. Measurement of Hardness and Elastic Modulus by Instrumented Indentation: Advances in Understanding and Refinements to Methodology. *J. Mater. Res.* **2004**, *19*, 3−20.
(30) Joslin, D. L.; Oliver, W. C. A New Method for Analyzing Data from Continuous Depth-Sensing Microindentation Tests. *J. Mater. Res.* **1990**, *5*, 123−126.
(31) Bobji, M. S.; Biswas, S. K.; Pethica, J. B. Effect of Roughness on the Measurement of Nanohardness-Computer Simulation Study. *Appl. Phys. Lett.* **1997**, *71*, 1059−1061.
(32) Tadjiev, D. R.; Hand, R. J. Calibrating a Nanoindenter for Very Shallow Depth Indentation Using Equivalent Contact Radius. *Philos. Mag.* **2010**, *90*, 1819−1832.
(33) Jian, S. R.; Jang, J. S. C.; Chen, G. J.; Chen, H. G.; Chen, Y. T. Nanoindentation on a-Plane ZnO Thin Films. *J. Alloys Compd.* **2009**, *479*, 348−351.
(34) Saha, R.; Nix, W. D. Effects of the Substrate on the Determination of Thin Film Mechanical Properties by Nanoindentation. *Acta Mater.* **2002**, *50*, 23−38.
(35) Kukli, K.; Ritala, M.; Sajavaara, T.; Keinonen, J.; Leskela, M. Atomic Layer Deposition of Hafnium Dioxide Films from Hafnium Tetrakis(ethylmethylamide) and Water. *Chem. Vap. Deposition* **2002**, *8*, 199−204.
(36) Tapily, K.; Jakes, J. E.; Stone, D. S.; Shrestha, P.; Gu, D.; Baumgart, H.; Elmustafa, A. A. Nanoindentation Investigation of HfO_2 and Al_2O_3 Films Grown by Atomic Layer Deposition. *J. Electrochem. Soc.* **2008**, *155*, H545−H551.